

A New Pyridine-3,4-dicarboxylic Acid Bridged Zinc(II) Coordination Complex: Crystal Structure, Quantum Chemistry and Luminescence Property^①

ZHAN Pei-Ying^a FENG Wan-Zhong^a LI Xiu-Mei^{a②} LIU Bo^{b②}

^a (Faculty of Chemistry, Tonghua Normal University, Tonghua 134002, China)

^b (Faculty of Chemistry, Jilin Normal University, Siping 136000, China)

ABSTRACT A new 2D metal coordination polymer, $[\text{Zn}(\text{pydc})(\text{L})(\text{H}_2\text{O})]_n \cdot 5n\text{H}_2\text{O}$ (**1**, H_2pydc = pyridine-3,4-dicarboxylic acid, L = 3-(2-pyridyl)pyrazole), was synthesized under hydrothermal conditions and characterized by single-crystal X-ray diffraction, powder XRD, FT-IR, thermogravimetric, fluorescence spectrum and elemental analysis techniques. Complex **1** belongs to the monoclinic system, $P2_1/c$ space group, with $a = 10.707(5)$, $b = 14.221(5)$, $c = 13.278(5)$ Å, $\beta = 102.071(5)^\circ$, $V = 1977.1(14)$ Å³ and $Z = 2$. It features a 2D network constructed by pydc^{2-} and L ligand. In addition, the quantum-chemical calculations were accomplished on ‘molecular fragments’ extracted from the crystal structure of **1** using the PBE0/LANL2DZ method built in Gaussian 16 Program. The calculation values denoted the distinct covalent interaction between the coordinated atoms and Zn(II) ion.

Keywords: coordination polymers, hydrothermal synthesis, crystal structure, luminescence property, quantum-chemical; DOI: 10.14102/j.cnki.0254-5861.2011-3092

1 INTRODUCTION

Owing to the unique structural tailorability and compositional diversity, metal coordination polymers (MCPs) have received much attention and become a hot topic due to their appealing applications as functional materials in adsorption separation, magnetism, luminescence, electrochemical sensors, and so on^[1]. The variety of the structures relies on the presence of suitable metal-ligand interactions and supramolecular contacts, which is directly related to the coordination characteristics of the components, such as the charge and radii of metal ions, the amount of dentate and steric hindrance of the ligands, etc^[2]. Although many MCPs with intriguing topologies have been reported, the control of precise structures of MCPs remains a great challenge in crystal engineering^[3].

The idea of mixed ligands can indeed obtain a great diversity of MCPs^[4]. However, the resulting structures are somewhat unpredictable and the governing principles in this

system are less ascertained and remain elusive^[5]. The organic pyridine-carboxylates as mixed ligand components are considered as a kind of remarkable building blocks in the construction of MCPs^[6]. They have the ability to balance charges, good coordination ability, and stability in acid and base. On the other hand, (pyridyl)pyrazole is a good organic ligand, which not only has various classes but also shows excellent coordination ability and spatial expansion ability in the process of assembling with metal ions^[7]. Thus, it is meaningful to investigate the effect of the combination of pyridine-carboxylates and heterocyclic (pyridyl)pyrazole mixed ligands on tuning the architectures of MCPs.

Based on the above consideration, a pyridine-3,4-dicarboxylic acid and a 3-(2-pyridyl)pyrazole were selected to react with Zn(II) ion under hydrothermal conditions. As a result, a 2D complex of $[\text{Zn}(\text{pydc})(\text{L})(\text{H}_2\text{O})]_n \cdot 5n\text{H}_2\text{O}$ (**1**), was obtained and structurally characterized by single-crystal X-ray diffraction, powder XRD, FT-IR, thermogravimetric, fluorescence spectrum, elemental analysis techniques and

Received 10 January 2021; accepted 1 March 2021 (CCDC 2054679)

① The project was supported by Jilin Science and Technology Development Program (JJKH20180776KJ) and Jilin Normal University Graduate Innovation Program (201939)

② Corresponding authors. Li Xiu-Mei, E-mail: lixm20032006@163.com; Liu Bo, E-mail: 112363305@qq.com

(Notes: These authors contribute equally to the work)

quantum-chemical calculations.

2 EXPERIMENTAL

2.1 Materials and methods

All starting materials purchased were of reagent quality and used without further purification. IR spectra (KBr pellets) and luminescence spectra were recorded on a Varian 640 FTIR spectrometer within the scope of $400 \sim 4000 \text{ cm}^{-1}$ and a Hitachi F-7000 fluorescence spectrometer at 296 K, respectively; powder X-ray diffraction and elemental analyses for C, N and H were performed with a D/teX Ultra diffractometer (40 kV and 40 mA, $\text{CuK}\alpha$) and a PE 2400C elemental analyzer, respectively.

2.2 Synthesis

A mixture of $\text{Zn}(\text{NO}_3)_2 \cdot 6\text{H}_2\text{O}$ (0.2 mmol, 0.0595 g), H_2pydc (0.20 mmol, 0.0334 g) and L (0.20 mmol, 0.029 g) was dissolved in 15 mL H_2O . Suitable amount of triethylamine was added to this solution to adjust the pH value to 7.03, followed by stirring at room temperature for 0.5 h until a homogeneous solution was obtained. Then it was sealed in a Parr Teflon-lined stainless-steel vessel (25 mL) under autogenous pressure at 170°C for 5 days. After cooling to room temperature, pale yellow block crystals of **1** suitable for X-ray diffraction were gained. Yield: 17% based on L. Elem. anal. calcd. for $\text{C}_{30}\text{H}_{20}\text{N}_8\text{O}_{19}\text{Zn}_2$: C, 38.86; H, 2.17; N,

12.08%. Found: C, 38.11; H, 1.98; N, 11.91%. IR (KBr, cm^{-1}): 3448(w), 3101(w), 1618(m), 1587(s), 1557(w), 1526(w), 1493(w), 1471(w), 1431(w), 1403(s), 1355(w), 1328(w), 1164(w), 1127(w), 1055(w), 1024(w), 982(w), 861(m), 840(m), 809(w), 780(w), 767(s), 718(m), 687(m), 650(w), 486(w), 462(w).

2.3 Determination of the crystal structures

A suitable single crystal of complex **1** was carefully selected under an optical microscope and data collection was performed on a Bruker D8 QUEST CMOS diffractometer with graphite-monochromatized $\text{MoK}\alpha$ radiation ($\lambda = 0.71073 \text{ \AA}$) using the ω -scan mode at room temperature. The raw data frames were integrated into SHELX-format reflection files and corrected using the SAINT program. Absorption corrections based on multi-scan were obtained using the SADABS program. All the structures were solved by direct methods and refined with full-matrix least-squares on F^2 using SHELXL-97^[8, 9]. Hydrogen atoms were located by geometric calculations and their positions and thermal parameters were fixed during the structure refinement. A total of 8836 reflections were collected in the range of $3.09 \leq \theta \leq 25.00^\circ$, of which 3412 were independent ($R_{\text{int}} = 0.1162$). The final $R = 0.0849$ and $wR = 0.1646$ for observed reflections with $I > 2\sigma(I)$, and $R = 0.1726$ and $wR = 0.2319$ for all data with $(\Delta\rho)_{\text{max}} = 1.131$ and $(\Delta\rho)_{\text{min}} = -1.130 \text{ e} \cdot \text{\AA}^{-3}$. Selected bond length and angle parameters are listed in Table 1.

Table 1. Selected Bond Lengths (\AA) and Bond Angles ($^\circ$) for **1**

Bond	Dist.	Bond	Dist.	Bond	Dist.
Zn(1)–O(2)	2.026(11)	Zn(1)–O(3A)	2.120(14)	Zn(1)–O(1W)	2.075(12)
Zn(1)–N(1)	2.161(14)	Zn(1)–N(2)	2.103(16)	Zn(1)–N(4B)	2.269(18)
Angle	($^\circ$)	Angle	($^\circ$)	Angle	($^\circ$)
O(2)–Zn(1)–O(1W)	96.9(5)	O(2)–Zn(1)–N(2)	92.8(5)	O(1W)–Zn(1)–N(2)	168.4(5)
O(2)–Zn(1)–O(3A)	89.3(5)	O(1W)–Zn(1)–O(3A)	87.9(5)	N(2)–Zn(1)–O(3A)	98.4(6)
O(2)–Zn(1)–N(1)	168.8(6)	O(1W)–Zn(1)–N(1)	93.0(6)	N(2)–Zn(1)–N(1)	76.8(6)
O(3A)–Zn(1)–N(1)	96.4(5)	O(2)–Zn(1)–N(4B)	86.6(5)	O(1W)–Zn(1)–N(4B)	87.4(6)
N(2)–Zn(1)–N(4B)	87.0(6)	N(1)–Zn(1)–N(4B)	88.5(6)		

Symmetry codes: (A) $-x+1, -y, z+1$; (B) $x, -y+1/2, z-1/2$

3 RESULTS AND DISCUSSION

3.1 Structural description

The single-crystal X-ray study reveals that complex **1**, $[\text{Zn}(\text{pydc})(\text{L})(\text{H}_2\text{O})]_n \cdot 5n\text{H}_2\text{O}$, consists of divalent Zn^{2+} ion, one pydc^{2-} anion, one L ligand, one coordination water molecule and five crystalline water molecules, as shown in Fig. 1, which also shows the coordination environments of $\text{Zn}(\text{II})$ ions and the ligands. Each Zn(1) ion in **1** is

six-coordinated by two N atoms from L chelating ligands, one N atom and two oxygen atoms from three bridging pydc^{2-} anions, and one coordination water molecule, in which the Zn(1)–O bond lengths are in the range of $2.026(11) \sim 2.120(14) \text{ \AA}$ and those of Zn(1)–N are from $2.103(16)$ to $2.269(18) \text{ \AA}$, which fall in the normal ranges and the coordination angles around the Zn ion vary from $76.8(6)$ to $173.4(6)^\circ$ ^[10].

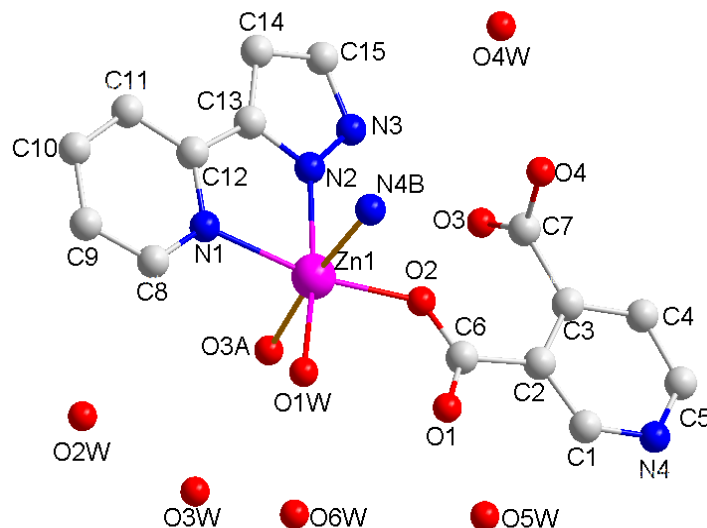


Fig. 1. Coordination environment of Zn(II) ion in **1**. Symmetry codes: (A) $-x+1, -y, z+1$; (B) $x, -y+1/2, z-1/2$

In complex **1**, each pydc^{2-} ligand adopts the μ_3 coordination mode, acting as a μ_3 -bridge to link four Zn(1) atoms, thus forming a two-dimensional network. It is different from our previous reported complex, $[\text{Ni}(\text{PDB})(\text{bix})(\text{H}_2\text{O})]_n^{[6(b)]}$, which was obtained by using the same pyridine-carboxylate and different nitrogenous ligands. Meanwhile, each L ligand adopts the μ_2 chelating coordination mode. Additionally, there are N-H \cdots O and C-H \cdots O hydrogen bonds derived from the pyrazol, pyridine and carboxylic groups. The hydrogen-bonding parameters of **1** are listed in Table 2. Moreover, there

exist π - π interactions between the pyridine ring of pydc^{2-} ligand and the imidazole ring of L ligand. The centroid distance is 3.623(11) Å for N(4)C(1)C(2)C(3)C(4)C(5) and N(2)N(3)C(15)C(14)C(13) rings (symmetry code: $1-x, -y, 1-z$), with the vertical distance to be 3.197(8) Å and the dihedral angle of 10°, indicating the existence of π - π interaction. The complex extends into a three-dimensional supramolecule (Fig. 2), so that it is more stable. From the view of topology, it takes a 2D net with a point symbol of $\{4^4 6^2\}$ (Fig. 3).

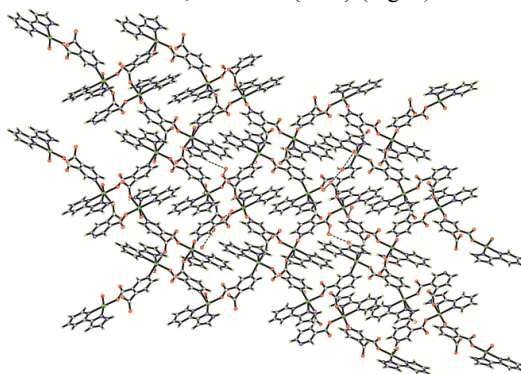


Fig. 2. View of the three-dimensional supramolecular structure along the a axis

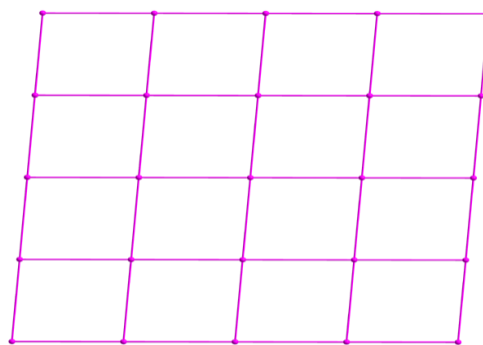


Fig. 3. 2D topological structure of **1**

3.2 IR analysis

IR spectra of **1** are shown in the frequency range of 400~4000 cm^{-1} (Fig. S1). The feature peak of -OH groups from water molecules of **1** is observed at about 3448 cm^{-1} [11]. The strong bands at about 1618 cm^{-1} for **1** are identified for $\nu_{\text{C=O}}$ vibration of the pydc²⁻ groups[12]. The peak located at 1403 cm^{-1} for **1** is attributed to the stretching vibration of carboxylic groups[13]. The strong bands in the region of 687~718 cm^{-1} can be assigned to the $\nu_{\text{C-N}}$ vibration of the N-heterocyclic rings of the ligands[14].

3.3 Powder X-ray diffraction (PXRD), and thermal stability analyses

The phase purity of the title complex was confirmed by comparison of its experimental powder X-ray diffraction (PXRD) pattern with the reference powder diffractogram (calculated from single-crystal X-ray diffraction data) (Fig. 4). The as-synthesized pattern agrees well with the corresponding simulated one, indicating that the phase purity of the sample is better. The difference in strength is due to the preferred orientation of the powder sample.

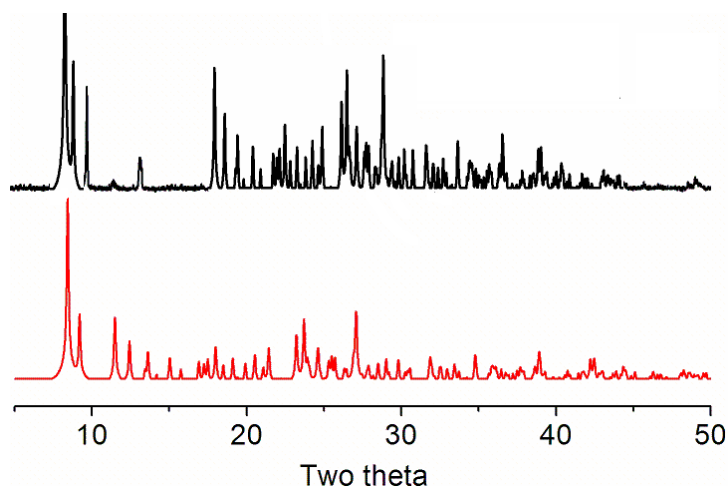


Fig. 4. PXRD analysis of **1**: bottom-simulated, top-experimental

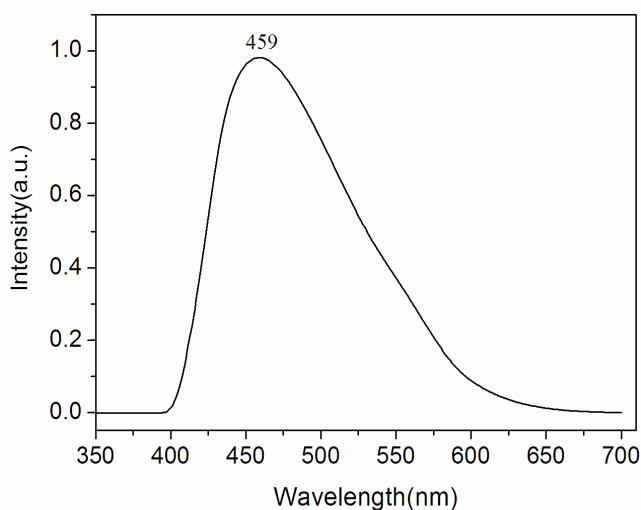


Fig. 5. Solid-state emission spectrum of **1** at room temperature

The thermal stability of complex **1** was investigated by thermogravimetric method using bulk materials under N_2 atmosphere of 20.0 $\text{mL} \cdot \text{min}^{-1}$ and 10 $^\circ\text{C} \cdot \text{min}^{-1}$. As shown in Fig. S2, the weight loss of 20.08% (calcd. 18.98%) for **1** from 87 to 181 $^\circ\text{C}$ is attributed to the release of water molecules, and 65.02% (calcd. 63.90%) from 181 to 505 $^\circ\text{C}$ belongs to the departure of L and pydc²⁻ ligands. The title complex can

be stable up to 475 $^\circ\text{C}$, following the decomposition of the framework.

3.4 Photoluminescent properties

Fig. 5 is a solid fluorescence diagram of complex **1** at room temperature. As can be seen from the diagram, upon excitation at 380 nm, complex **1** shows a broad emission peak at 459 nm. The strongest emission peak of H_2pydc is around

370 nm, mainly due to the $\pi^* \rightarrow n$ transition of ligand^[15]. Therefore, the emission peak of complex **1** can not be caused by $\pi^* \rightarrow n$ transition of H₂pydc. And the 3-(2-pyridyl)pyrazole molecule has a strong emission peak at about 443 nm at room temperature. By consulting literature^[16, 17], the fluorescence of complex **1** is neither produced by the charge transition from metal to ligand, nor the charge transition from ligand to metal, but generated electronic transitions within the 3-(2-pyridyl)pyrazole ligand. Compared with the fluorescence of 3-(2-pyridyl)pyrazole molecules, the emission spectra of complex **1** exhibit red shifts of ca. 16 and enhanced fluorescence intensity, which is mainly due to the formation of complex. The metal-ligand coordination increases the rigidity of the system, reduces the energy loss due to vibration and enhances the fluorescence intensity.

4 QUANTUM CHEMISTRY CALCULATIONS

All calculations in this manuscript were performed with the Gaussian16 program^[18]. The parameters of the molecular fragments for calculation were extracted from the crystal structure of the title complex. Natural bond orbital (NBO)

analysis was performed by density functional theory (DFT)^[19] with the PBE0^[20-23] hybrid functional and the LANL2DZ basis set^[24].

The selected atom net charges, electron configuration, Wiberg bond and NBO bond orders (a.u) of the title complex are listed in Table 2. The calculation results indicate that the electronic configuration of Zn(II) ion is $4s^{0.29}3d^{9.98}4p^{0.30}$, and those of N and O atoms are $2s^{1.32-1.33}2p^{4.00-4.20}$ and $2s^{1.66-1.70}2p^{5.10-5.29}$. Based on the above values, the Zn(II) ion coordination with N and O atoms is mainly on 3d, 4s and 4p orbitals. N atoms form coordination bonds with Zn(II) ion using 2s and 2p orbitals. All O atoms supply electrons of 2s and 2p to Zn(II) ion and form the coordination bonds. Therefore, the Zn(II) ion obtained some electrons from three N atoms of L and three O atoms of pydc²⁻ ligand^[25]. Thus, according to valence-bond theory, the atomic net charge distribution and the NBO bond orders of the title complex (Table 3) show obvious covalent interaction between the coordinated atoms and Zn(II) ion. The differences of the NBO bond orders for Zn–O and Zn–N make their bond lengths different^[26], which is in good agreement with the X-ray crystal structural data of the title complex.

Table 2. Hydrogen Bonds for Complex 1

D–H···A	d(D–H)	d(H···A)	d(D···A)	∠(DHA)	Symmetry codes
N(3)–H(3A)···O(3)	0.86	2.17	3.01(2)	165	
C(1)–H(1A)···O(1)	0.93	2.39	2.73(2)	102	
C(5)–H(5A)···O(4)	0.93	2.51	3.44(2)	171	<i>x</i> , 1/2– <i>y</i> , 1/2+ <i>z</i>
C(11)–H(11A)···O(1)	0.93	2.58	3.45(3)	156	1– <i>x</i> , –1/2+ <i>y</i> , 1/2– <i>z</i>

Table 3. Selected Atom Net Charges, Electron Configurations, Wiberg Bond Indexes and NBO Bond Orders of 1

Atom	Net charge	Electron configuration	Bond	Wiberg bond index	NBO bond order
Zn(1)	1.29893	[core]4s(0.29)3d(9.98)4p(0.42)			
O(1W)	–0.99330	[core]2s(1.70)2p(5.29)	Zn(1)–O(1W)	0.1630	0.2390
O(2)	–0.81066	[core]2s(1.66)2p(5.14)	Zn(1)–O(2)	0.2250	0.2262
O(3A)	–0.76973	[core]2s(1.66)2p(5.10)	Zn(1)–O(3A)	0.2540	0.2846
N(1)	–0.54025	[core]2s(1.32)2p(4.20)	Zn(1)–N(1)	0.1648	0.2576
N(2)	–0.35201	[core]2s(1.32)2p(4.00)	Zn(1)–N(2)	0.1782	0.2262
N(4B)	–0.48061	[core]2s(1.33)2p(4.12)	Zn(1)–N(4B)	0.1368	0.2197

As can be seen from Fig. 6, the LUMO (the lowest unoccupied molecular orbital) and HOMO (the highest occupied molecular orbital) electron clouds are mainly located

at the L ligand. Therefore, ILCT may be inferred from some contours of molecular orbital of the title complex.

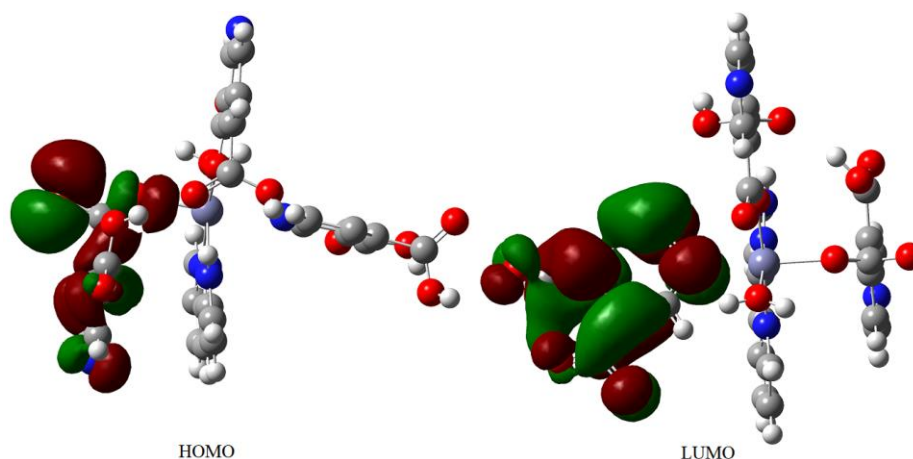


Fig. 6. Frontier molecular orbitals of 1

REFERENCES

- (1) (a) Eddaoudi, M.; Moler, D. B.; Li, H. L.; Chen, B. L.; Reineke, T. M.; O'Keeffe, M.; Yaghi, O. M. From molecules to crystal engineering: supramolecular isomerism and polymorphism in network solids modular chemistry: secondary building units as a basis for the design of highly porous and robust metal-organic carboxylate frameworks. *Acc. Chem. Res.* **2001**, 34, 319–330.
- (b) Li, H. L.; Eddaoudi, M.; O'Keeffe, M.; Yaghi, O. M. Design and synthesis of an exceptionally stable and highly porous metal organic framework. *Nature* **1999**, 402, 276–279.
- (c) Feltham, H. L. C.; Brooker, S. Review of purely 4f and mixed-metal nd-4f single-molecule magnets containing only one lanthanide ion. *Coord. Chem. Rev.* **2014**, 276, 1–33.
- (d) Zhao, D.; Cui, Y. J.; Yang, Y.; Qian, G. D. Sensing-functional luminescent metal-organic frameworks. *CrystEngComm*. **2016**, 18, 3746–3759.
- (e) Cui, J. W.; Hou, S. X.; Li, Y. H.; Cui, G. H. A multifunctional Ni(II) coordination polymer: synthesis, crystal structure and applications as a luminescent sensor, electrochemical probe, and photocatalyst. *Dalton Trans.* **2017**, 46, 16911–16924.
- (2) (a) Gao, Q.; Xu, J.; Bu, X. H. Recent advances about metal-organic frameworks in the removal of pollutants from wastewater. *Coord. Chem. Rev.* **2019**, 378, 17–31.
- (b) Yang, D. D.; Liu, Y.; Li, S. S.; Cheng, L.; Wang, Y.; Zhang, Y. X.; Chen, K.; Gao, Y. X.; Ren, P.; Day, G. S.; Wang, Y. Ligand-rearrangement-induced transformation from a 3D supramolecular network to a discrete octanuclear cluster: a good detector for Pb²⁺ and Cr₂O₇²⁻. *ACS Omega* **2019**, 4, 11493–11499.
- (c) Zhang, J. W.; Kan, X. M.; Liu, B. Q.; Liu, G. C.; Tian, A. X.; Wang, X. L. Systematic investigation of reaction-time dependence of three series of copper-lanthanide/lanthanide coordination polymers: syntheses, structures, photoluminescence, and magnetism. *Chem. Eur. J.* **2015**, 21, 16219–16228.
- (3) (a) Lee, J. Y.; Farha, O. K.; Roberts, J.; Scheidt, K. A.; Nguyen, S. T.; Hupp, J. T. Metal-organic framework materials as catalysts. *Chem. Soc. Rev.* **2009**, 38, 1450–1459.
- (b) Qian, J.; Sun, M. M.; Liu, M.; Gu, W. Macromolecular probe based on a Ni^{II}/Tb^{III} coordination polymer for sensitive recognition of human serum albumin (HSA) and MnO₄⁻. *ACS Omega*. **2019**, 4, 11949–11959.
- (c) Wang, J.; Gao, L. L.; Zhang, J.; Zhao, L.; Wang, X. Q.; Niu, X. Y.; Fan, L. M.; Hu, T. P. Syntheses, gas adsorption, and sensing properties of solvent-controlled Zn(II) pseudo-supramolecular isomers and Pb(II) supramolecular isomers. *Cryst. Growth Des.* **2019**, 2, 630–637.
- (4) (a) Li, X. M.; Sun, M.; Pan, Y. R. Synthesis, crystal structure and theoretical calculations of a nickel(II) coordination polymer assembled by 4,4'-oxydibenzoic acid and 1,3-bis(imidazol-1-ylmethyl)-benzene ligands. *Chin. J. Struct. Chem.* **2015**, 34, 710–718.
- (b) Li, X. M.; Pan, Y. R.; Liu, B.; Zhou, S. Syntheses, crystal structures and theoretical calculations of two complexes of cadmium assembled by bis(imidazol) ligands. *Chin. J. Inorg. Chem.* **2019**, 35, 1275–1282.
- (c) Li, X. M.; Wang, Z. T.; Pan, Y. R.; Wang, Q. W.; Liu, B. Synthesis, crystal structure and theoretical calculations of two zinc, cobalt coordination polymers with 5-nitroisophthalic acid and 1,4-bis(1H-benzimidazolyl)butane ligands. *J. Inorg. Organomet. Poly.* **2018**, 28, 258–267.
- (d) Pan, Y. R.; Li, X. M.; Ji, J. Y.; Wang, Q. W. Synthesis, crystal structure, and theoretical calculations of two cobalt, nickel coordination polymers with 5-nitroisophthalic acid and bis(imidazol) ligands. *Aust. J. Chem.* **2016**, 69, 1296–1304.

- (5) (a) Kirchon, A.; Feng, L.; Drake, H. F.; Joseph, E. A.; Zhou, H. C. From fundamentals to applications: a toolbox for robust and multifunctional MOF materials. *Chem. Soc. Rev.* **2018**, 23, 8611–8638.
- (b) Fang, W. H.; Yang, G. Y. Induced aggregation and synergistic coordination strategy in cluster organic architectures. *Acc. Chem. Res.* **2018**, 11, 2888–2896.
- (c) Fan, L. M.; Zhang, Y. J.; Liang, J. F.; Wang, X. Q.; Lv, H. X.; Wang, J.; Zhao, L.; Zhang, X. T. Structural diversity, magnetic properties, and luminescence sensing of five 3D coordination polymers derived from designed 3,5-di(2',4'-dicarboxylphenyl)benzoic acid. *CrystEngComm.* **2018**, 20, 4752–762.
- (6) (a) Li, X. M.; Wang, Q. W.; Liu, B. Synthesis and crystal structure of a new nickel(II) complex with 2,4-pyridinedicarboxylic acid and 1,4-bis(imidazol-1-ylmethyl)-benzene ligands. *Chin. J. Struct. Chem.* **2012**, 31, 889–893.
- (b) Wang, Q. W.; Guo, J.; Lu, T. F.; Li, X. M.; Liu, B.; Wang, Z. T. Hydrothermal synthesis and crystal structure of a new nickel(II) complex with 3,4-pyridinedicarboxylic acid and 1,4-bis(imidazol-1-ylmethyl)-benzene ligands. *Chin. J. Struct. Chem.* **2012**, 31, 1575–1579.
- (c) Liu, G. C.; Li, Y.; Chi, J.; Xu, N.; Wang, X. L.; Lin, H. Y.; Chen, Y. Q. Multi-functional fluorescent responses of cobalt complexes derived from functionalized amide-bridged ligand. *Dyes Pigments* **2020**, 174, 108064(1–7).
- (7) (a) Li, X. M.; Pan, Y. R.; Zhan, P. Y.; Wang, Q. W.; Liu, B. A new Cd(II) coordination polymer constructed by 3-(2-pyridyl)pyrazole and 5-nitroisophthalic acid: synthesis, crystal structure and theoretical calculations. *Chin. J. Struct. Chem.* **2017**, 36, 1609–1616.
- (b) Wang, X. Y.; Li, X. M.; Pan, Y. R.; Liu, B.; Zhou, S. A new three-dimensional Cd(II) complex assembled by 1,3,5-benzenetricarboxylic acid and 3-(2-pyridyl)pyrazole. *Chin. J. Struct. Chem.* **2019**, 38, 1275–1282.
- (8) Sheldrick, G. M. *SHELXS 97, Program for the Solution of Crystal Structure*. University of Göttingen, Germany **1997**.
- (9) Sheldrick, G. M. *SHELXL 97, Program for the Refinement of Crystal Structure*. University of Göttingen, Germany **1997**.
- (10) Wang, Z. T.; Valtchev, V.; Fang, Q. R.; Li, X. M.; Pan, Y. R. Hydrothermal synthesis and crystal structure of three-dimensional supramolecular zinc, manganese coordination polymers. *Inorg. Nano-met. Chem.* **2019**, 49, 44–50.
- (11) Zhu, L. N.; Deng, Z. P.; Huo, L. H.; Gao, S. Cd(II) coordination polymers constructed from bis(pyridyl) ligand with asymmetric chelating spacer and diverse organic dicarboxylates: syntheses, structural evolutions and properties. *Dalton Trans.* **2019**, 48, 7589–7601.
- (12) Yang, L.; Wang, F.; Auphedeous, D. Y.; Feng, C. L. Achiral isomers controlled circularly polarized luminescence in supramolecular hydrogels. *Nanoscale* **2019**, 11, 14210–14215.
- (13) Wang, X. L.; Mu, B.; Lin, H. Y.; Liu, G. C. Three new two-dimensional metal-organic coordination polymers derived from bis(pyridinecarboxamide)-1,4-benzene ligands and 1,3-benzenedicarboxylate: syntheses and electrochemical property. *J. Organomet. Chem.* **2011**, 696, 2313–2321.
- (14) Dolensky, B.; Konvalinka, R.; Jakubek, M.; Kral, V. Identification of intramolecular hydrogen bonds as the origin of malfunctioning of multitopic receptors. *J. Mol. Struct.* **2013**, 1035, 124–128.
- (15) (a) Chen, S. S.; Zhao, Y.; Fan, J.; Okamura, T.; Bai, Z. S.; Chen, Z. H.; Sun, W. Y. Construction of coordination frameworks based on 4-imidazolyl tecton 1,4-di(1H-imidazol-4-yl)benzene and varied carboxylic acids. *CrystEngComm.* **2012**, 14, 3564–3576.
- (b) Zang, S. Q.; Su, Y.; Li, Y. Z.; Ni, Z. P.; Meng, Q. J. Assemblies of a new flexible multicarboxylate ligand and d^{10} metal centers toward the construction of homochiral helical coordination polymers: structures, luminescence, and NLO-active properties. *Inorg. Chem.* **2006**, 1, 174–180.
- (16) Wen, L.; Lu, Z.; Lin, J.; Tian, Z.; Zhu, H.; Meng, Q. Syntheses, structures, and physical properties of three novel metal-organic frameworks constructed from aromatic polycarboxylate acids and flexible imidazole-based synthons. *Cryst. Growth Des.* **2007**, 7, 93–99.
- (17) Lin, J. G.; Zang, S. Q.; Tian, Z. F.; Li, Y. Z.; Xu, Y. Y.; Zhu, H. Z.; Meng, Q. J. Metal-organic frameworks constructed from mixed-ligand 1,2,3,4-tetra-(4-pyridyl)-butane and benzene-polycarboxylate acids: syntheses, structures and physical properties. *CrystEngComm.* **2007**, 9, 915–921.
- (18) Frisch, M. J.; Trucks, G. W.; Schlegel, H. B.; Scuseria, G. E.; Robb, M. A.; Cheeseman, J. R.; Stratmann, R. E.; Yazyev, O.; Austin, A. J.; Cammi, R.; Pomelli, C.; Ochterski, J. W.; Ayala, P. Y.; Morokuma, K.; Voth, G. A.; Salvador, P.; Dannenberg, J. J.; Zakrzewski, V. G.; Dapprich, S.; Daniels, A. D.; Strain, M. C.; Farkas, O.; Malick, D. K.; Rabuck, A. D.; Raghavachari, K.; Foresman, J. B.; Ortiz, J. V.; Cui, Q.; Baboul, A. G.; Clifford, S.; Cioslowski, J.; Stefanov, B. B.; Liu, G.; Liashenko, A.; Piskorz, P.; Komaromi, I.; Martin, R. L.; Fox, D. J.; Keith, T.; AlLaham, M. A.; Peng, C. Y.; Nanayakkara, A.; Challacombe, M.; Gill, P. M. W.; Johnson, B.; Chen, W.; Wong, M. W.; Gonzalez, C.; Pople, J. A. *Gaussian16*, revision B.16; Gaussian, Inc., Pittsburgh, PA **2016**.
- (19) Parr, R. G.; Yang, W. *Density Functional Theory of Atoms and Molecules*. Oxford University Press: Oxford **1989**.

- (20) Ernzerhof, M.; Scuseria, G. E. Assessment of the Perdew-Burke-Ernzerhof exchange-correlation functional. *J. Chem. Phys.* **1999**, 110, 5029–5036.
- (21) Adamo, C.; Barone, V. Toward reliable density functional methods without adjustable parameters: the PBE0 model. *J. Chem. Phys.* **1999**, 110, 6158–6170.
- (22) Perdew, J. P.; Burke, K.; Ernzerhof, M. Generalized gradient approximation made simple. *Phys. Rev. Lett.* **1996**, 77, 3865–3868.
- (23) Perdew, J. P.; Burke, K.; Ernzerhof, M. Generalized gradient approximation made simple. *Phys. Rev. Lett.* **1997**, 78, 1396–1397.
- (24) Dunning, T. H. Jr.; Hay, P. J. In *Modern Theoretical Chemistry*. Schaefer HF, III, Ed.; Plenum: New York **1976**, 3, 1–28.
- (25) Wang, L.; Zhao, J.; Ni, L.; Yao, J. Synthesis, structure, fluorescence properties, and natural bond orbital (NBO) analysis of two metal [Eu^{III}, Co^{II}] coordination polymers containing 1,3-benzenedicarboxylate and 2-(4-methoxyphenyl)-1H-imidazo[4,5-f][1,10]phenanthroline ligands. *ZAAC*. **2012**, 638, 224–230.
- (26) Li, Z. P.; Xing, Y. H.; Zhang, Y. H. Synthesis, structure and quantum chemistry calculation of scorpionate oxovanadium complexes with benzoate. *Acta Phys. Chim. Sin.* **2009**, 25, 741–746.